

PAPER • OPEN ACCESS

## Research of Influence of the Shape of Unreinforced Masonry Shear Walls Made of Calcium Silicate Masonry Units

To cite this article: Radoslaw Jasinski 2019 *IOP Conf. Ser.: Mater. Sci. Eng.* **471** 022009

View the [article online](#) for updates and enhancements.

### Recent citations

- [Research of Behaviour of Bed Joints Reinforced Masonry Walls with Openings Made of Autoclaved Aerated Concrete under Horizontal Shearing](#)  
Radoslaw Jasinski

# Research of Influence of the Shape of Unreinforced Masonry Shear Walls Made of Calcium Silicate Masonry Units

Radosław Jasinski <sup>1</sup>

<sup>1</sup> Department of Building Structures, Silesian University of Technology,  
Akademicka 5, 44-100 Gliwice, Poland

radoslaw.jasinski@polsl.pl

**Abstract.** We performed tests on 6 calcium silicate masonry units which were laid in thin layer mortar with uneven head joints. Walls were divided into two series and denoted by convention as HOS (Jasiński 2016) and HOS-H. Those two series differed in overall dimensions of test elements. Three walls from HOS series had identical external dimensions:  $l = 4.50$  m,  $h = 2.45$  m ( $h/l = 2.45\text{m}/4.50\text{m}$ ), and thickness  $t = 180$  mm. The walls were tested at different values of initial compressive stress  $\sigma_c = 0; 0.1; 1.0$  and  $1.5$  N/mm<sup>2</sup>. The HOS-H elements were prepared as unreinforced test elements with the length  $l = 2.25$  m height  $h = 2.45$  m ( $h/l = 2.45\text{m}/2.25$  m) and thickness  $t = 0.18$  m, and tested at initial compressive stress equal to  $\sigma_c = 0.1; 0.75; 1.5$  N/mm<sup>2</sup>. The tests showed that the wall shape had a negligible effect on the morphology of cracks and the failure mechanism. An increase in wall length caused a roughly proportional increase in values of cracking and failure stresses. Shorter walls were under considerably greater cracking and failure stresses. An increase in wall length led to a significant decrease in values of shear strain angle regardless of initial compressive stress. The reverse situation occurred at the moment of destruction. Values of shear strain then increased with an increasing length of the wall.

## 1. Introduction

The problems related to shear walls are intrinsically linked to issues of stiffening walls. In terms of design, such problems are solved *by analogy* to constructions with walls made of reinforced concrete [1]. But that solution takes into account specificity of the wall caused by, inter alia, its non-homogeneous and orthotropic structure and low tensile strength. Complexity of the aspect of shear masonry structures makes the simple theoretical or analytical models of little use without research verification. Therefore, the aim of this paper is to introduce the behaviour of masonry walls with different shapes, subjected to simultaneous compressive and horizontal shear stress. According to theoretical analyses [2, 3], proportions between height and length of the wall determine its strength and stiffness. The discussed tests are the continuation of the author's research tests, whose earlier stages included [4, 5, 6, 7] walls made of solid brick. This paper presents walls made of calcium silicate masonry units, which were partially described in the paper [8].



## 2. Test models and testing technique

We performed tests on 6 calcium silicate masonry units which were laid in thin layer mortar with uneven head joints. Compressive strength of masonry (according to PN-EN 1052-1:2000 [9]) was  $f_{c,mv} = 11.3 \text{ N/mm}^2$ , and the modulus of elasticity was  $E_{cm} = 7833 \text{ N/mm}^2$ . Shear strength determined according to PN-EN 1052-3:2004 [10] was  $f_{vo} = 0.70 \text{ N/mm}^2$ , and shear modulus for walls under diagonal tension (according to ASTM E519-81 [11]) was  $G_{cr} = 895 \text{ N/mm}^2$ . The walls were divided into two series and denoted by convention as HOS (Figure 1a) and HOS-H (Figure 1b). Those two series differed in overall dimensions of specimens. Three walls from HOS series had identical external dimensions:  $l = 4.50 \text{ m}$ ,  $h = 2.45 \text{ m}$  ( $h/l = 2.45\text{m}/4.50\text{m}$ ), and thickness  $t = 180 \text{ mm}$ . Three unreinforced walls from HOS series were tested at three different values of initial compressive stress  $\sigma_c = 0; 0.1; 1.5 \text{ N/mm}^2$ . HOS-H elements were prepared as unreinforced test elements with the length  $l = 2.25 \text{ m}$ , height  $h = 2.45 \text{ m}$  ( $h/l = 2.45\text{m}/2.25\text{m}$ ) and thickness  $t = 0.18 \text{ m}$ . They were tested at initial compressive stress equal to  $\sigma_c = 0.1; 0.75; 1.5 \text{ N/mm}^2$ .

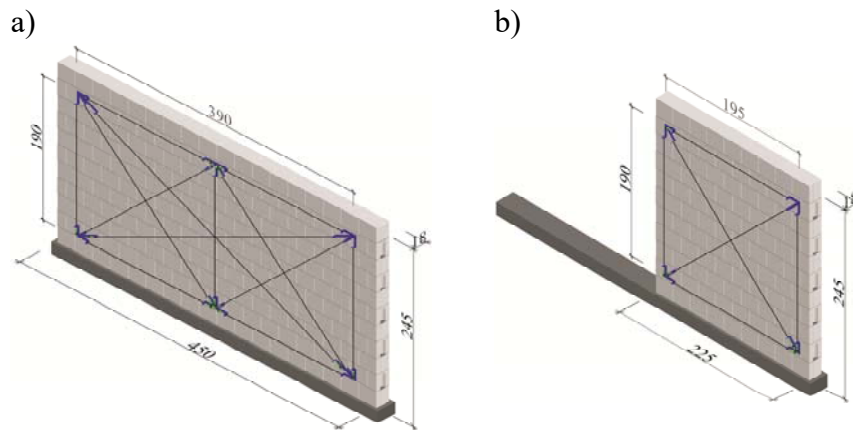


**Figure 1.** Geometry of models: a) walls from HOS series, length 4.5 m, b) walls from HOS-H series, length 2.25 m

The author tested walls at the test stand previously used for brick walls [4, 5, 6, 7]. The test stand was designed and modified to adapt it to walls with the maximum length of 4.5 m and the height of ca. 2.5 m. The stand provided the option of forcing horizontal shear force with the maximum capacity of 3000 kN and applying simultaneously vertical compressive load with the maximum force of 1250 kN. The details of the test stand were described in e.g. the paper [8, 12]. A frame structure was used to measure shear angle. The structure was fixed to both sides of the test model. As it was planned to measure stiffness of the whole wall, the size of the frame measurement system was chosen to include the maximum area of the wall, and at the same time to neglect edge disorders. The measuring system was firmly fixed to the wall surface using epoxy adhesive. The system was symmetrically fixed to both sides of the test model that the diagonal centre of the test model corresponded to the diagonal centre of the frame system – Figure 2.

We measured displacements ( $\Delta_c, \Delta_f, \Delta_i, \Delta_j, \Delta_g, \Delta_h$ ) along each side (c, f, i, j) of the test model and along two diagonals (g, h) of the frame system, using inductive converters of displacement PJX-20 with the accuracy of 0.002 mm. The range of indications was  $\pm 10 \text{ mm}$ . Knowing changes in lengths of sides (at  $i^{\text{th}}$  level of loading) ( $l_{cc}, l_{fc}, l_{ic}, l_{jc}$ ) and diagonals ( $l_{gc}, l_{hc}$ ), we could determine partial angles of shear strain  $\Theta_j$  ( $j = 1, 2, 3, 4$ ) which were theoretically separated from the deformed measuring system.

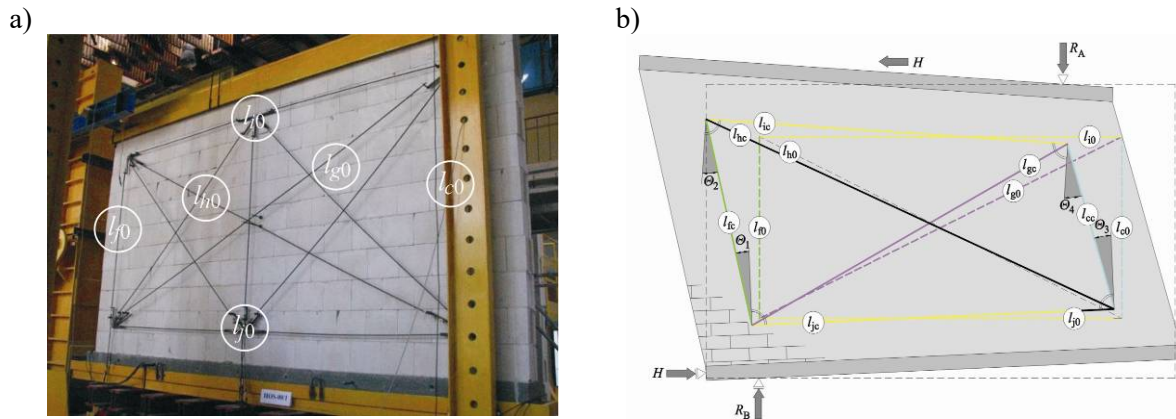


**Figure 2.** The frame system for measuring shear strain angles: a) the wall made of calcium silicate masonry units, b) symbols of measuring bases and partial angles of shear strain

The terms **general angle of shear strain** or **general angle of shear deformation** in the phase after cracking were used to describe the wall behaviour under horizontal loading. Partial values of the general angle of shear strain  $\Theta_j$  were determined according to the law of cosines, on the basis of average changes in the length of measuring bases (Figure 2b). For example, for a triangle with the sides  $l_{fc}$ ,  $l_{hc}$ ,  $l_{jc}$  the shear strain angle was expressed by the following relationship:

$$l_{hc}^2 = l_{fc}^2 + l_{jc}^2 - 2l_{fc}l_{jc} \cos\left(\frac{\pi}{2} + \Theta_1\right) \rightarrow \Theta_1 = -\frac{\pi}{2} + \arccos\left(\frac{l_{fc}^2 + l_{jc}^2 - l_{hc}^2}{2l_{fc}l_{jc}}\right). \quad (1)$$

The length of measuring bases under the load was determined from the following relationships:  $l_{ic} = l_{i0} + \Delta_i$ ,  $l_{jc} = l_{j0} + \Delta_j$ ,  $l_{cc} = l_{c0} + \Delta_c$ ,  $l_{fc} = l_{f0} + \Delta_f$ ,  $l_{gc} = l_{g0} + \Delta_g$ ,  $l_{hc} = l_{h0} + \Delta_h$ . The average value of the **general angle of shear strain** of the masonry  $\Theta$ , (at  $i^{\text{th}}$  level of loading) was determined as the mean arithmetic value of partial values  $\Theta_j$

$$\Theta = \frac{1}{n} \left( \sum_{j=1}^{n=4} |\Theta_j| \right). \quad (2)$$

Shear stress  $\tau_i$  was determined as the ratio of horizontal loading  $H_i$  and the horizontal area of the masonry in accordance with the following relationship:

$$\tau_{v,i} = \frac{H_i}{A_h}. \quad (3)$$

**General stiffness of a wall**  $K_i$  was the ratio of the applied force  $H_i$  and the corresponding horizontal displacement  $u_i$  according to the following relationship

$$K_i = \frac{H_i}{u_i} = \frac{\tau_i}{\Theta_i} \frac{A_h}{h}. \quad (4)$$

The wall stiffness at the moment of observing first cracks was denoted as  $K_{cr}$ . Initial stiffness  $K_o$  was determined in the initial phase of loading at stress values  $0 < \tau \leq 0.05\tau$ . The measured force, at which the first crack was observed in the masonry units or mortar was considered as the cracking force  $H_{cr}$ . The corresponding stresses  $\tau_{cr}$ , were defined as cracking stresses, and the angle  $\Theta_{cr}$  was defined as the shear strain angle at the moment of cracking. The width of 0.1 mm was regarded as the minimum width of the crack, neglecting all previously observed micro-cracks. I prepared a detailed list of existing and visible cracks in the masonry units to avoid any wrong interpretations of visible cracks. The measured force, at which the model was destroyed was considered as the destructive force  $H_u$  – an

increase in force was not further recorded at increasing displacements. Stresses at the top edge of the wall, corresponding to the force  $H_u$  were regarded as failure stresses  $\tau_{cr}$ , and the angle  $\Theta_u$  as shear strain deformation angle. Because the testing accessories obstructed the access to the masonry face, I did not update the list of cracks, but only observed their behaviour (the place of formation, direction of propagation).

### 3. Test results

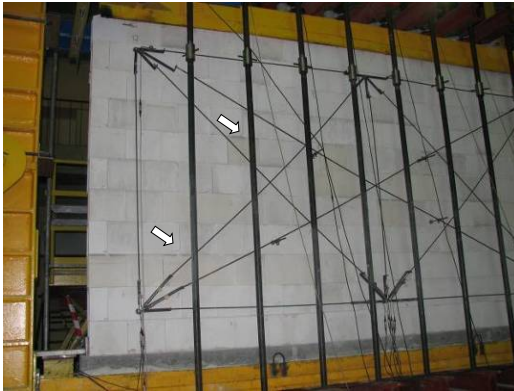
#### 3.1. The cracking mechanism in the models

The cracking process in walls without openings from HOS series (the longest walls) was similar. First diagonal cracks were formed almost simultaneously near the supports A and B. Horizontal cracks in the central part of the wall were developed almost at the same time. The increased loading caused that the cracks in the top and bottom part of the wall joined the cracks from the central part of the masonry, forming a wide crack. In the elements subjected to minimal shear and compressive stress, there was a single diagonal and horizontal crack running through bed and head joints at the interface between the masonry units. Single diagonal cracks running through the masonry units were formed at the top edge of the wall. In the wall under maximum shear and compressive stress, the cracks were developed in the area close to the supports and in the central part of the masonry. The increased shear load caused that diagonal cracks propagated towards bottom and top edge of the wall. First cracks visible in unreinforced elements from HOS series, subjected to maximum and minimum compressive stress, were shown in Figures. 3a and 3b.

Apart from original cracks propagating towards opposite wall edges, in the unreinforced wall subjected to minor compressive stresses and increasing load, we observed new diagonal cracks at the opposite corners of the wall, running through bed and head joints. At the moment of destruction, there was one diagonal crack running through bed and head joints (Figure 4a). In the central part of the wall, it joined the horizontal crack in the bed joint. At the same time a few masonry units in the top layer were crushed. In the unreinforced wall under maximum shear and compressive stress, diagonal cracks were running along the whole height of the wall, that is, through head joints and masonry units (Figure 4b). In the walls from HOS-H series, which were shorter by 50% than the walls from HOS series, the scheme of cracks formation was similar. In the wall under minimum shear and compressive stress, the first crack in the bed joint was formed in the central part of the wall, at the support B – Figure 5a. In the walls compressed to the value of  $0.75 \text{ N/mm}^2$  and  $1.50 \text{ N/mm}^2$ , first cracks were observed in the central part of the wall – Figures 5b, c. Unlike in the wall under minimum compressive stress, the cracks did not run through bed and head joints, but through the masonry units.

An increase in shear loading applied to the unit under minimum compressive stress developed the first crack along the wall diagonal, and two additional and parallel cracks that ran through bed and head joints – Figure 6a. At the moment of destruction, additional diagonal cracks were noticed in the individual masonry units at the highest layer of the wall. In the wall compressed to the initial value of  $0.75 \text{ N/mm}^2$  an increase in the shear loading developed the diagonal crack which covered almost the total length of the wall diagonal – Figure 6b. No additional cracks were noticed. In the third wall under maximum compressive load of  $1.50 \text{ N/mm}^2$  I observed at the moment of destruction the initial crack which covered the whole diagonal of the wall, many diagonal cracks near vertical supports, and horizontal cracks in the central part of the wall – Figure 6c.

a)



b)

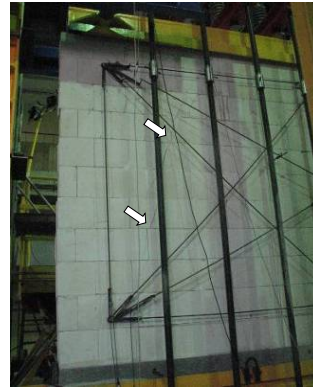
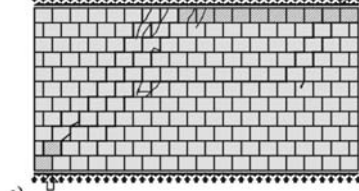


**Figure 3.** First visible cracks in walls from HOS series: a) shear wall under initial compressive stress  $\sigma_c = 0 \text{ N/mm}^2$ , b) shear wall at  $\sigma_c = 1.5 \text{ N/mm}^2$

a)



b)

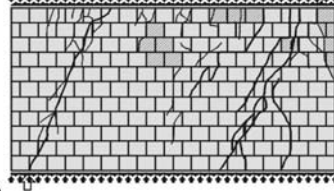
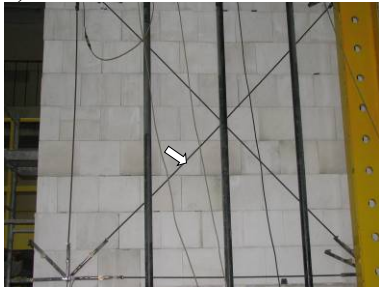


**Figure 4.** Cracking of wall models from HOS series at the moment of destruction: a) shear wall at  $\sigma_c = 0.1 \text{ N/mm}^2$ , b) shear wall at  $\sigma_c = 1.5 \text{ N/mm}^2$

a)



b)



c)

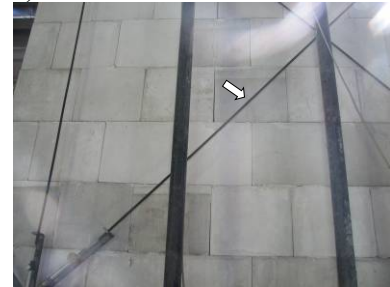


**Figure 5.** First visible cracks in walls from HOS-H series: a) shear wall at  $\sigma_c = 0.1 \text{ N/mm}^2$ , b) shear wall at  $\sigma_c = 0.75 \text{ N/mm}^2$ , c) shear wall at  $\sigma_c = 1.5 \text{ N/mm}^2$



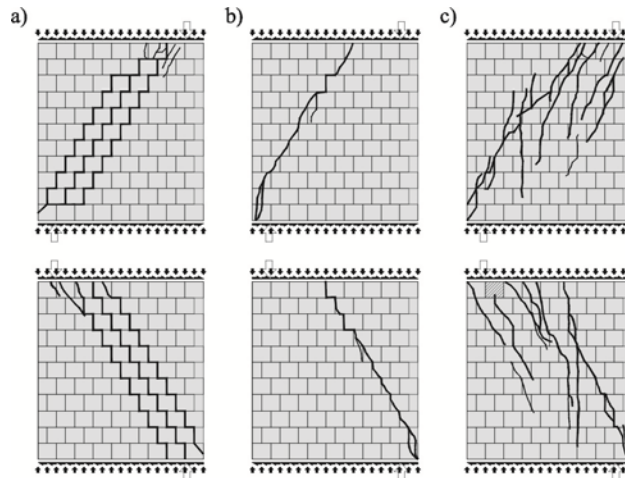


**Figure 6.** Cracking of wall models from HOS-H series at the moment of destruction: a) shear wall at  $\sigma_c = 0.1 \text{ N/mm}^2$ , b) shear wall at  $\sigma_c = 0.75 \text{ N/mm}^2$  c) shear wall at  $\sigma_c = 1.5 \text{ N/mm}^2$

### 3.2. Stress-strain relationships

Figure 7 illustrates the relationships between stress  $\tau_{v,i}$  and strain  $\theta_i$  for the test elements from HOS and HOS-H series. Figure 8 shows the obtained changes in the total stiffness of walls from HOS and HOS-H series.

The relationships determined during the tests indicated that stress-shear strain angle relationship was nearly directly proportional until the moment of destruction. In HOS-15/1 models under maximum compressive stress, after cracking (slightly breaking of the line on the graph) I could observe wall strengthening and further increase in the value of shear strain angle at an increasing shear loading. A further increase in horizontal loading resulted in slight strengthening of the wall. Apart from noticeably lower values of shear stress, the stress-shear deformation relationship for HOS-H walls with the shortest length were nearly the same. An increase in shear deformations was proportional until the moment of destruction. In the walls compressed to 0.75 and 1.5  $\text{N/mm}^2$ , I could observe their strengthening after cracking. Also in the wall compressed to 0.10  $\text{N/mm}^2$ , its strengthening after previous cracking was noticeable, and the shear deformation at the moment of destruction was twice as high as in the walls under compressive stress.

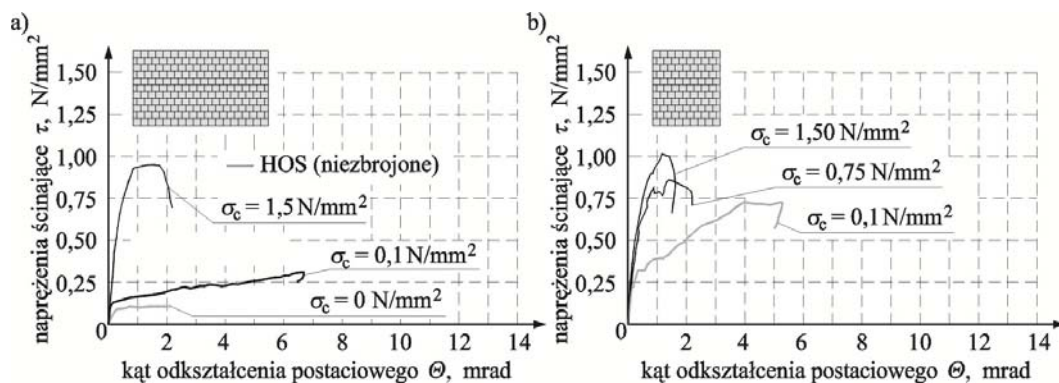


**Figure 7.** Shear stress-angle of shear deformation relationship for the walls made of calcium silicate units: a) test elements from HOS series ( $l=4.50 \text{ m}$ ), b) test elements from HOS-H series ( $l=2.25 \text{ m}$ )

There was a clear degradation of shear modulus for the walls from series HOS (Figure 8a) at an increasing values of shear stress, and inverse proportional relationship  $K-\tau$  was observed. The biggest drop in initial stiffness  $K_0$  was identified in the range of shear stresses  $0.1\tau_u - 0.1 \text{ N/mm}^2$ . At further

increase in the shear loading, the drop in stiffness values was considerably lower. However, in shorter test elements from HOS-H series (Figure 8b), subjected to shear stress at the values of compressive stress 0.1 and 0.75 N/mm<sup>2</sup>, the degradation in initial stiffness of the walls was much smaller in comparison to longer test elements. In the test element subjected to the same maximum shear and compressive stress like the model HOS-15/1, there was a rapid drop in stiffness at loading inducing the shear stresses  $0.1\tau_u - 0.1 \text{ N/mm}^2$ . The changes in stiffness were subtle at a further increase in shear stress.

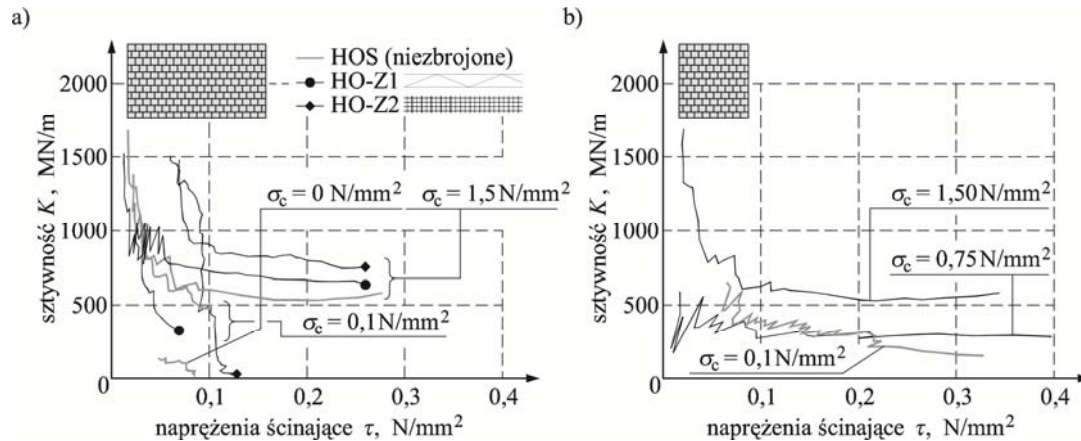


**Figure 8.** Stiffness-shear stress relationship for the walls made of calcium silicate units: a) test elements from HOS series ( $l=4.50 \text{ m}$ ), b) test elements from HOS-H series ( $l=2.25 \text{ m}$ )

Table 1 presents the obtained test results expressed as shear stresses determined at the moment of cracking  $\tau_{cr}$  and destruction  $\tau_u$  on the basis of the following formula (3). There are also general angles of shear strain for the walls corresponding to cracking stress  $\theta_{cr}$  and angles of shear deformation corresponding to failure stress  $\theta_u$ , determined from the following formulas (1), (2). The table also includes the obtained values of initial total stiffness  $K_0$  (taking into account bending and shear strains) at shear stresses  $0.1-0.3\tau_u$  and at the moment of wall cracking  $K_{cr}$  determined from the following formula (4).

**Table 1.** Test results

Series ( $l \times h \times t$ )	Type of reinforcement	$\rho_{th}, \%$	$\sigma_c$ N/mm <sup>2</sup>	Stresses		Angles of shear strain (deformation)		Total stiffness	
				cracking	failure	cracking	failure	initial	at the moment of cracking
				$\tau_{cr}$ N/mm <sup>2</sup>	$\tau_u$ N/mm <sup>2</sup>	$\theta_{cr}$ mrad	$\theta_u$ mrad	$K_0$ MN/m	$K_{cr}$ MN/m
HOS (4.5×2.45 ×0.18m)	NO REINFORCEMENT	0	0	0.069	0.107	0.175	2.126	137	131
			0.1	0.124	0.313	0.086	6.714	1378	477
			1.5	0.346	0.954	0.197	2.182	1674	580
HOS-H (2.25×2.4 5×0.18m)	NO REINFORCEMENT	0	0.1	0.327	0.74	0.370	4.97	645	146
			0.75	0.552	0.88	0.356	2.21	587	257
			1.5	0.913	1.04	0.785	1.61	1635	192

### 3.3. Effect of wall shape

The effect of wall shape on mechanical parameters was only analysed for unreinforced walls. The analysis included the reference walls from HOS series (with the length of 4.50 m and the height of 2.45 m) and from HOS-H series having the identical height and the length equal to 1/2 length of the reference walls. The walls from each series were tested at stresses equal to  $\sigma_c = 0.1$  and  $1.5 \text{ N/mm}^2$ . Figure 9 illustrates the comparison of values of shear stress at the moment of cracking and destruction



of all types of walls. The discussed relationships indicated that the increase in initial values of compressive stress caused an increase in values of cracking stress. Within the range of initial compressive stresses, the highest cracking stress was observed in the shortest elements from HOS-H series. At the moment of destruction, failure stress was increasing proportionally to an increase in initial compressive stress. Also shorter elements at the moment of destruction had lower values of shear stress in comparison to the reference elements from HOS series. We observed the inverse tendency when  $\sigma_c$  series were increasing.

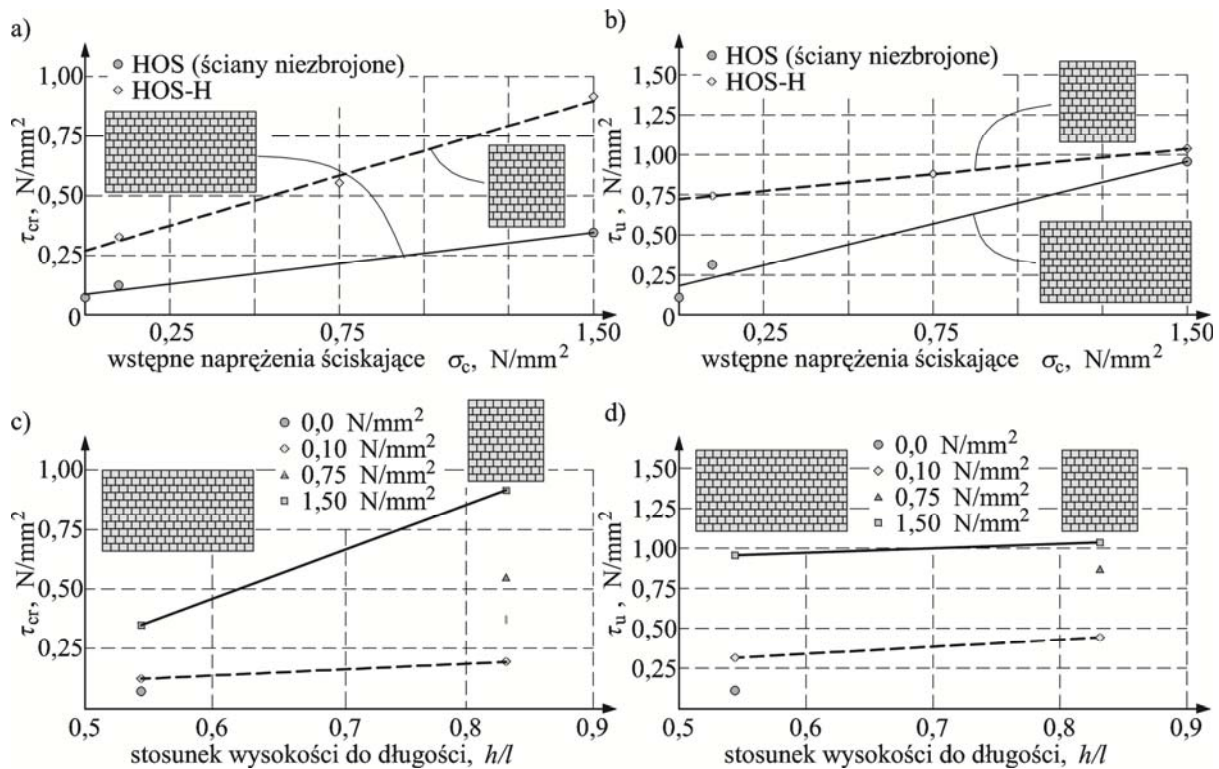


**Figure 9.** The obtained (cracking and failures) stress values for all test elements depending on the value  $\sigma_c$  and the wall shape: a), c) cracking stresses –  $\tau_{cr}$ , b), d) failure stresses –  $\tau_{cr}$

Figure 10 illustrates the comparison of values of shear strain angle at the moment of cracking and shear strain deformation angle at the moment of destruction of all types of walls.

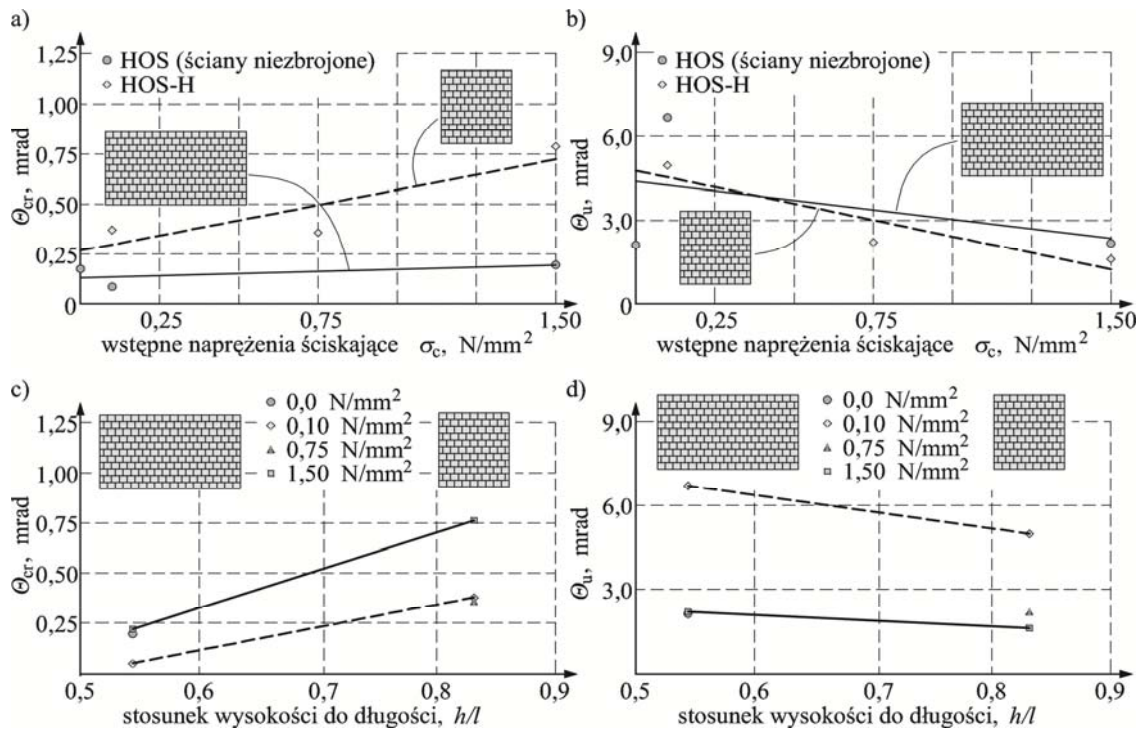


**Figure 10.** The obtained angles of shear strain and deformation at the moment of cracking and destruction of all test elements depending on the value  $\sigma_c$  and the wall shape: a), c) shear strain angle at the moment of cracking –  $\Theta_{cr}$ , b), d) shear deformation at the moment of destruction –  $\Theta_u$

Like in case of shear stress, the initial compressive stress caused an increase in deformation angles. In the shortest walls, at the zero value of compressive stress, the extrapolated angle of shear deformation was ca. 0.25 mrad. An increase in initial values of compressive stress caused an apparent increase in the values of shear deformation in the wall under maximum compressive load up to the level of 0.75 mrad. In the reference shear walls, to which no maximum compressive stress was applied, shear deformation was ca. 0.1 mrad and an increase in initial compressive stress did not cause a noticeable increase in shear deformation. Angles of shear deformation at the moment of destruction were reduced while the values of initial compressive stress were increasing. At stress 0.1 N/mm<sup>2</sup> the destruction was observed at deformation of ~4.5 mrad. And at stress 1.5 N/mm<sup>2</sup> the shear deformation reached the value of ca. 2 mrad. Figure 11 compares total initial stiffness and stiffness at the moment of cracking.

The total stiffness of walls at the moment of cracking was increasing with an increase in values of initial compressive stress. The longest walls demonstrated the highest values of stiffness and a greater increase in stiffness. Initial stiffness of walls was decreasing with an increase in values of compressive stress. Like in case of stiffness  $K_{cr}$ , the values of initial stiffness of walls were also increasing. Longer walls also had greater stiffness. A reduced length of walls resulted in a nearly proportional decrease in stiffness.

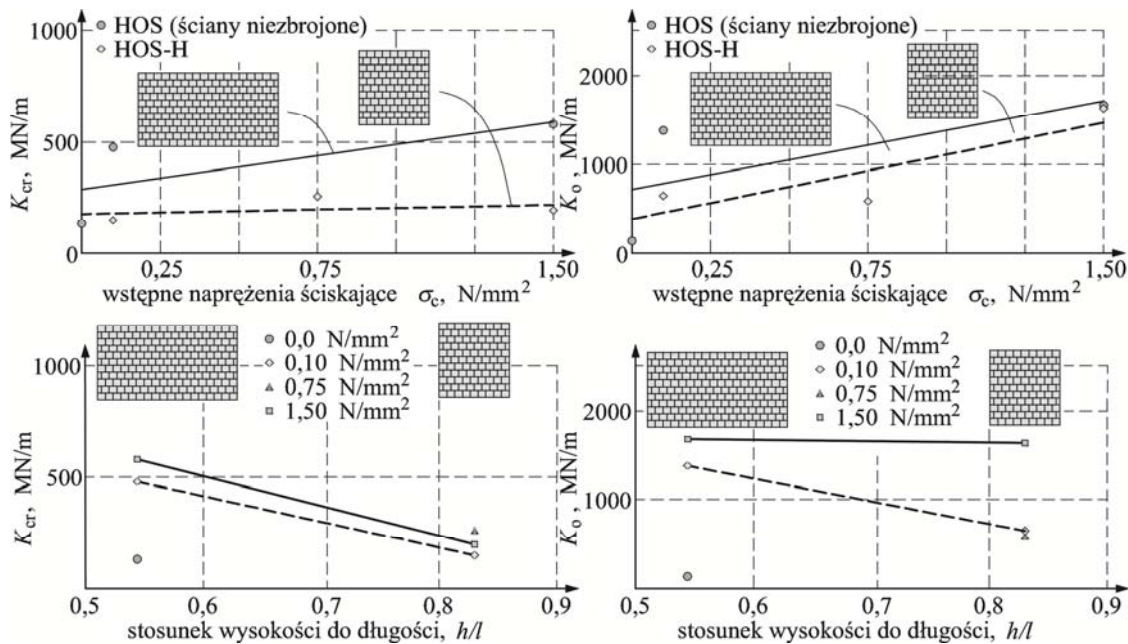


**Figure 11.** The obtained stiffness values for all test elements depending on the value  $\sigma_c$  and the wall shape: a), c) stiffness at the moment of cracking –  $\tau_{cr}$ , b), d) initial stiffness –  $\tau_{cr}$

#### 4. Conclusions

The performed tests on unreinforced walls of two different shapes lead to the following conclusions:

The observed methods of shear wall destruction indicate that:

- regardless of the wall length, first cracks were formed near supports and in the central part of the wall. Cracks were larger in longer walls compared to more slender ones, Initial compressive stress was the most significant factor affecting crack morphology. In walls subjected to minimum compressive stress, there was a predominant single crack running through head and bed joints, whereas in walls subjected to maximum compressive stress, including masonry units, there were many diagonal, and even vertical cracks.

Regarding shear strain angles at the moment of cracking  $\theta_{cr}$  and destruction  $\theta_u$ , the following observations were made:

- there was a noticeable impact of initial compressive stress, like in the paper [3]. In the unreinforced walls in maximum compression, stress values  $\tau_{cr}$  increased by more than 180% in comparison to the walls under minimum compressive stress ( $\sigma_c = 0.1 \text{ N/mm}^2$ ). The similar situation referred to failure stress  $\tau_u$  which increased in the walls from HOS series by more than 200%, and in the walls from HOS-H series up to nearly 40%,
- longer walls caused a nearly proportional increase in cracking and failure stress values [2, 3]. Shorter walls were under considerably greater cracking and failure stresses.

Regarding shear strain angles at the moment of cracking  $\theta_{cr}$  and destruction  $\theta_u$ , the following observations were made:

- the effect of initial compressive stress was similar to shear stress, but only for angles of shear deformation at the moment of cracking. In HOS walls under maximum compression,  $\theta_{cr}$  values increased by 129%, and in shorter walls by 112%. At the moment of destruction,  $\theta_u$  values in the longest walls under maximum compressive stress were lower by 67% than in the walls under minimum compressive stress, on which the tests were performed in the same way. Also in shorter walls from HOS-H series, shear deformation was lower by 68% than in case of the walls under minimum compressive load of  $0.1 \text{ N/mm}^2$ ,

- values of shear strain angles noticeably decreased as the wall length increased, regardless of initial compressive stress values. The reverse situation occurred at the moment of failure. Values of shear strain then increased along with increasing length of the wall.

Considering the initial stiffness  $K_0$  and stiffness at the moment of cracking  $K_{cr}$ , it was found that:

- the effect of initial compressive stress values was the most important for HOS-H walls. In the walls under maximum compressive stress, initial stiffness  $K_0$  increased by more than 153%, and by more than 20% in the reference walls under minimum compressive stress. For stiffness values determined at the moment of cracking,  $K_{cr}$  stiffness increased by more than 20% in the longest walls under maximum compressive stress. For HOS-H walls, stiffness under maximum compressive stress was lower by 32%.

## References

- [1] A.W. Hendry, B.P. Sinha, S.R. Davies, „Design of Masonry Structures”. E&FN SPON, 2004. Third edition.
- [2] S. Petrovčič S, V. Kilar, „Seismic failure mode interaction for the equivalent frame modeling of unreinforced masonry structures”, *Engineering Structures*, Vol. 54, 2013, pp. 9-22.
- [3] L. Songbo, A.N. Fried, J. J. Roberts, „Cracking of Brickwork Shear Walls”, *Proceedings of 4<sup>th</sup> International Masonry Conference*. British Masonry Society Proceedings No. 7, London 1995, Vol. 1, pp. 134-139.
- [4] R. Jasiński R, „Strenght and deformability of reinforced clay brick masonry horyzonatally sheared”. *PhD Thesis*. Silesian University of Technology, Gliwice, Poland 2005. DOI. 10.13140/RG.2.2.29271.68001. (In Polish)
- [5] R. Jasiński, „Study of reinforced clay brick masonry walls horizontally sheared”, *8<sup>th</sup> International Masonry Conference*, Dresden 2010, pp. 1231–1242.
- [6] Ł. Drobiec, R. Jasiński, A. Piekarczyk, I. Galman, „Research of clay brick walls in the different load states”. *Inżynieria i Budownictwo*, Nr 5-6/2010, pp. 315–322, ISSN 0021-0315. (In Polish)
- [7] R. Jasiński, „Research of reinforced clay brick sheared horyzontally”. *Przegląd Budowlany*, Nr 9/2009, pp. 28–36, ISSN 0033-2038. (In Polish).
- [8] R. Jasiński, „Research of bed joints reinforced masonry walls with openings made of calcium silicate units horizontally sheared”. *Brick and Block Masonry – Trends, Innovations and Challenges*. Taylor & Francis Group, London 2016, pp. 2303 - 2311.
- [9] PN-EN 1052-1:2000 Methods of tests for masonry. Part 1: Determination of Compression Strenght. (In Polish)
- [10] PN-EN 1052-3:2004 Methods of tests for masonry. Part 3: Determination of Initial Shear Strenght. (In Polish)
- [11] ASTM E519-81 Standard Test Method for Diagonal Tension (Shear) of Masonry Assemblages.
- [12] R. Jasiński, „Research and modeling of masonry shear walls”. *PhD DsC Thesis*. Silesian University of Technology, Gliwice, Poland 2017. (In Polish)